

## DYNAMICS OF RADIATIVE SUPERNOVA REMNANTS

DENIS F. CIOFFI

Department of Astronomy, University of California at Berkeley

CHRISTOPHER F. MCKEE

Departments of Physics and Astronomy, University of California at Berkeley

AND

EDMUND BERTSCHINGER

Department of Physics, Massachusetts Institute of Technology

Received 1987 June 10; accepted 1988 April 25

### ABSTRACT

Guided by a new, higher resolution numerical simulation, we have taken a fresh look at the evolution of a supernova remnant (SNR) evolving in a homogeneous, uniform medium. We have concentrated on the transition from the adiabatic stage to the radiative pressure-driven snowplow stage, and the possible further establishment of a momentum-conserving snowplow stage. In the numerically simulated example (ejecta mass of  $3 M_{\odot}$ , ambient hydrogen density of  $0.1 \text{ cm}^{-3}$ ), the radiative stage begins after less than one sound crossing time from the end of the free-expansion stage, and as a result the interior of the blast wave never completely settles to the Sedov-Taylor similarity solution. After the adiabatic stage the expansion does not follow a power law in time.

Using an equation of motion for the blast wave taken from Ostriker and McKee, we derive a set of simple ordinary differential equations which correctly reproduce the kinematics of the blast wave seen in the numerical simulation. The simple pressure-driven snowplow solution ( $R_s = \text{constant } t^{2/7}$ ) is found not to provide a correct description of the expansion during the radiative epoch due to the “memory” of the extra pressure in that stage. A simple “offset” power law,  $R \propto (t - t_{\text{offset}})^{3/10}$ , describes the numerical results for the radiative stage. We demonstrate that in most cases the momentum-conserving snowplow ( $R \propto t^{1/4}$ ) is delayed beyond the merger of the remnant with the interstellar medium.

*Subject headings:* hydrodynamics — nebulae: supernova remnants — shock waves

### I. INTRODUCTION

After the highly energetic ( $\approx 10^{51}$  ergs of kinetic energy) explosion which accompanies a supernova, the ejected material drives a blast wave into the ambient interstellar medium (ISM) to produce a supernova remnant (SNR). The physical configuration of the remnant changes several times throughout the evolution, and so the expansion is generally characterized in terms of several stages (e.g., Woltjer 1972). If we insist that the expansion obey a power law in time  $t$ , where the shock radius  $R_s \propto t^n$ , and  $t$  is measured from the time of the explosion, we can loosely identify these stages by the value of the exponent  $n$ .

The mass and momentum of the ejected material initially dominate the evolution, and in this free-expansion  $\eta_{ej} = 1$ . In addition to the shock pushing ahead of the ejecta into the ISM, a reverse-shock also propagates back into the ejecta (e.g., McKee 1974). In this paper we shall consider the continuous evolution of the remnant only after it enters the next stage, where the swept-up material dominates the remnant mass. Then we expect the familiar Sedov-Taylor stage (ST) (Sedov 1959; Taylor 1950), with an adiabatic shock, a self-similar, adiabatic interior, and  $\eta \equiv \eta_{ST} = \frac{2}{5}$ .

The first parcel of shocked material to cool completely does so at  $t_{sf}$ , when a thin shell forms which “snowplows” through the ISM, driven by the pressure of the hot, roughly isobaric interior in addition to its own momentum (Cox 1972; Chevalier 1974). Somewhat before  $t_{sf}$ , at  $t_{PDS}$ , as the effective ratio of specific heats begins to approach 1 and the postshock fluid velocity approaches the shock velocity, we say that the radi-

ative or *pressure-driven snowplow* (PDS) stage of evolution has begun. In the absence of interior cooling, the standard analytic solutions find  $R_s \propto t^{2/7}$  (McKee and Ostriker 1977).

Although the interior gas loses energy by pushing the shell through the ISM, previous analytic treatments of the PDS stage have not allowed for interior energy loss from radiation. If we account for this interior radiation (Kahn 1976), we eventually recover Oort’s solution (Oort 1951), the *momentum-conserving snowplow* (MCS), with  $R_s \propto t^{1/4}$ . The final evolution occurs when the shock velocity drops to about the sound speed of the surrounding gas, with the presumed breakup of the shell, and the remnant merges with the ISM.

In this paper we examine SNR evolution with two goals in mind: (1) to understand the discrepancies between numerical simulations and the standard analytic treatment, in particular with regard to the dynamics of the pressure-driven snowplow stage and a possible transition to the momentum-conserving snowplow stage; and (2) to show a simple analytic structure which will reproduce the kinematical evolution of a supernova remnant through all stages. In particular, this allows an accurate calculation of the luminosity from the fully radiative shock,  $L \propto R_s^2 v_s^3$ .

We shall describe the evolution of an idealized SNR within the following framework: (a) negligible pressure, either gas or magnetic, in the surrounding material, until the transition to the last, merger stage; (b) a spherical expansion (i.e., a one-dimensional evolution); (c) a homogeneous ISM (no clouds); (d) a uniform ISM (no density gradients); (e) negligible cooling by dust (Ostriker and Silk 1973; Dwek 1981; Graham *et al.*

1987). (*f*) no thermal conduction (see, e.g., Solinger, Rappaport, and Buff 1975; Cox and Edgar 1983).

In the next section we present the results from a numerical simulation of an explosion in a medium with a hydrogen density of  $0.1 \text{ cm}^{-3}$ . In § III we provide a simple physical model for the overall dynamics and present our analytic approximations, good to a few percent in radius and velocity when compared with the numerical simulations. In a companion paper (Cioffi and McKee 1988), we derive general solutions for the kinematics and luminosity from SNRs in all stages of evolution.

## II. NUMERICAL SIMULATION OF SUPERNOVA REMNANT EVOLUTION

Using a spherically symmetric explicit Lagrangian hydrodynamics code, we have studied the evolution of a supernova remnant from the ejecta stage, into the adiabatic stage, and through the radiative snowplow stages. The simulations and results are similar to those of Chevalier (1974), Straka (1974), Mansfield and Salpeter (1974), Falle (1981), and others, but have much higher resolution, allowing a more precise comparison of the results to simple models of remnant evolution. In this section we discuss the numerical methods and present the results.

The numerical code integrates the equations of gas dynamics with spherical symmetry. These equations yield the evolution of the mass density  $\rho$ , radial velocity  $v$ , and pressure  $P$ :

$$\frac{d\rho}{dt} = -\rho \frac{1}{r^2} \frac{\partial}{\partial r} (r^2 v), \quad (2.1)$$

$$\frac{dv}{dt} = -\frac{1}{\rho} \frac{\partial P}{\partial r}, \quad (2.2)$$

$$\frac{dP}{dt} = -\gamma P \frac{1}{r^2} \frac{\partial}{\partial r} (r^2 v) - (\gamma - 1)n^2 \Lambda(T), \quad (2.3)$$

where  $(d/dt) = (\partial/\partial t) + v(\partial/\partial r)$  is the usual Lagrangian time derivative,  $n$  is the hydrogen density, and the cooling function  $\Lambda(T)$  is defined such that  $n^2 \Lambda$  gives the luminosity per unit volume. Grid points are moved using the auxiliary equation  $dr/dt = v$ . We treat the gas as ideal, with a ratio of specific heats  $\gamma = 5/3$  and a temperature  $T$  determined from  $P = \rho k_B T/\mu$ , where  $k_B$  is Boltzmann's constant and  $\mu$  is the mean molecular weight. Only a single gas component is evolved and we treat  $\mu = (14/23)m_H$  as constant, corresponding to complete ionization of a gas with composition  $n_{He}/n = 0.10$ .

Our treatment of the thermodynamics is simplified in several respects, but we argue that this has no effect on the global evolution of the remnant. The function  $\Lambda(T)$  which was used in the numerical simulation is a piecewise power-law fit to the results of Raymond, Cox, and Smith (1976) for optically thin cooling from a gas of solar abundance in collisional ionization equilibrium. This cooling law is not correct inside the thin radiative shell that forms after the ST stage ends because the gas is not in ionization equilibrium; the gas also absorbs the UV radiation produced in the shell (Chevalier 1974). Thus our results do not correctly give the detailed structure within the radiative shell. However, these details are irrelevant to the global evolution of the blast wave as long as the shell remains thin (Bertschinger 1986). In our simulations the shell becomes so thin that it proved necessary to truncate radiative cooling below a temperature  $T_c$ , initially  $1.2 \times 10^4 \text{ K}$ , to prevent the

dynamical and cooling time scales from becoming too short in the shell. Chevalier (1974) achieved the same end by adding a term to the fluid equations representing approximately the effects of magnetic fields. We neglect magnetic fields but note that they are important for the global evolution only if they inhibit formation of a thin shell. We note that heat conduction, if not inhibited by magnetic fields, could change some of our quantitative results because it would lead to enhanced cooling of the hot interior gas owing to losses from evaporation of cold gas in the radiative shell.

To integrate numerically the fluid equations (2.1)–(2.3), the fluid variables were first evaluated on a discrete Lagrangian grid  $r_i(t)$  ( $i = 1, 2, \dots, N$ ). Radial derivatives were evaluated by fitting and differentiating a cubic spline through the grid points. This procedure reduces the partial differential fluid equations to a series of coupled ordinary differential equations for the time-dependence of the fluid variables evaluated at the grid points. These equations were advanced in time using an explicit three-stage integrator illustrated here for the equation  $dr_i/dt = v_i$ , where  $r_i^n \equiv r_i(t^n)$ ,  $\Delta t \equiv t^{n+1} - t^n$ :

$$r'_i = r_i^n + \frac{\Delta t}{2} v_i^n, \quad r''_i = r'_i + \Delta t v'_i,$$

$$r_i^{n+1} = r''_i + \frac{\Delta t}{2} (v_i^n - 2v'_i + v''_i). \quad (2.4)$$

The fluid equations were advanced in the form of equations (2.1)–(2.3) rather than in the Eulerian conservation-law form because a Lagrangian treatment (or a complicated regridding algorithm) is necessary to resolve adequately the high-density radiative shell. The time step  $\Delta t$  is constrained by the shorter of the Courant time step, which is determined by the sound-crossing time from one grid point to the next (Richtmyer and Morton 1967), and the cooling time scale. Without the third stage the scheme of equations (2.4) would be a second-order Runge-Kutta algorithm, which is unstable for hyperbolic systems such as the fluid equations; this last stage stabilizes the method. The integrator is second-order accurate in time; no significant differences were found (other than a decrease in speed) when a four-stage, fourth-order Runge-Kutta integrator was used. It is common wisdom that high-order methods such as cubic splines and Runge-Kutta integrators are a poor choice for computational hydrodynamics with shocks, but in our experience these methods are more robust and flexible than lower-order methods. With considerable effort one can design a method superior to the one adopted here (e.g., Collella and Woodward 1984), but our algorithm proved satisfactory in the present application.

The treatment of shocks requires the addition of numerical artificial viscosity to the method described above. Artificial viscosity terms based on the ordinary linear shear viscosity of a compressible gas,  $\eta_{\text{vis}}$ , (Landau and Lifshitz 1959) were added to the momentum and energy equations (2.2) and (2.4), as follows:

$$\rho \frac{\partial v}{\partial t} = \frac{1}{r^2} \frac{\partial}{\partial r} \left[ \frac{4}{3} \eta_{\text{vis}} r^2 \left( \frac{\partial v}{\partial r} - \frac{v}{r} \right) \right] + \frac{4}{3} \frac{\eta_{\text{vis}}}{r} \left( \frac{\partial v}{\partial r} - \frac{v}{r} \right),$$

$$\frac{\rho}{(\gamma - 1)} \frac{\partial}{\partial t} \left( \frac{p}{\rho} \right) = \frac{4}{3} \eta_{\text{vis}} \left( \frac{\partial v}{\partial r} - \frac{v}{r} \right)^2. \quad (2.5)$$

Rather than using the molecular viscosity of a gas, we choose  $\eta_{\text{vis}}$  using characteristic grid length and time scales so that the

highest frequency numerical oscillations would be damped in a few time steps. Equations (2.5) were implemented as a fractional time step using finite differences (Lapidus 1967); this treatment assures that the artificial viscosity does not change the Courant stability condition and does not affect the numerical conservation of mass and energy. Much experimentation yielded a form of the viscosity coefficient proportional to the first central velocity difference divided by the local sound speed; this choice results in viscous dissipation being applied near shocks (where velocity changes are rapid) but not in the smooth parts of a flow. The method was applied to standard shock tube problems (Sod 1978) and to an adiabatic point explosion (the ST solution), with excellent agreement: with a grid of  $N = 100$  divisions, mass and energy are conserved to better than 1%, the fluid variables are accurate to  $\sim 1\%$  in the smooth flow regions, and the shock width is  $\sim 3$  grid spacings (the last is independent of  $N$ ).

The initial conditions used for the simulations of supernova remnant evolution were as follows. A supernova explosion energy of  $0.931 \times 10^{51}$  ergs was deposited in the kinetic energy of  $3 M_{\odot}$  of stellar ejecta. The ejecta were taken to be of solar abundance and have uniform density; while this is unrealistic it

has no significant effect on the blast wave evolution after the remnant enters the adiabatic stage. The interstellar density, also of solar abundance, was  $n = 0.1 \text{ cm}^{-3}$ . The interstellar temperature was set to 10 K so that the blast wave remained strong throughout the simulation. The numerical simulations began at  $t = 170$  yr after the explosion, when the ejecta overdensity was a factor of 100. A contact discontinuity separates the ejecta from the interstellar gas. The initial grid spacing was 0.1 pc in the interstellar gas and 10 times finer in the ejecta. The total number of grid points was  $N = 1327$ . Throughout the simulation, of total duration  $1.75 \times 10^6$  yr, mass and energy were conserved to relative errors of 0.047% and 1.8%, respectively.

Figures 1–4 show the fluid variables plotted versus radius at several times of interest. The dynamics of the remnant evolution is sufficiently interesting that we provide a detailed discussion here before addressing the overall rate of expansion of the remnant, which was the primary motivation for the simulation.

Figure 1 shows the fluid variables at  $t = 1.2 \times 10^5$  yr, roughly  $2.5 \times t_{\text{PDS}}$  (eq. [3.11]), the beginning of the radiative stage. By this time 20% of the initial energy has been lost to

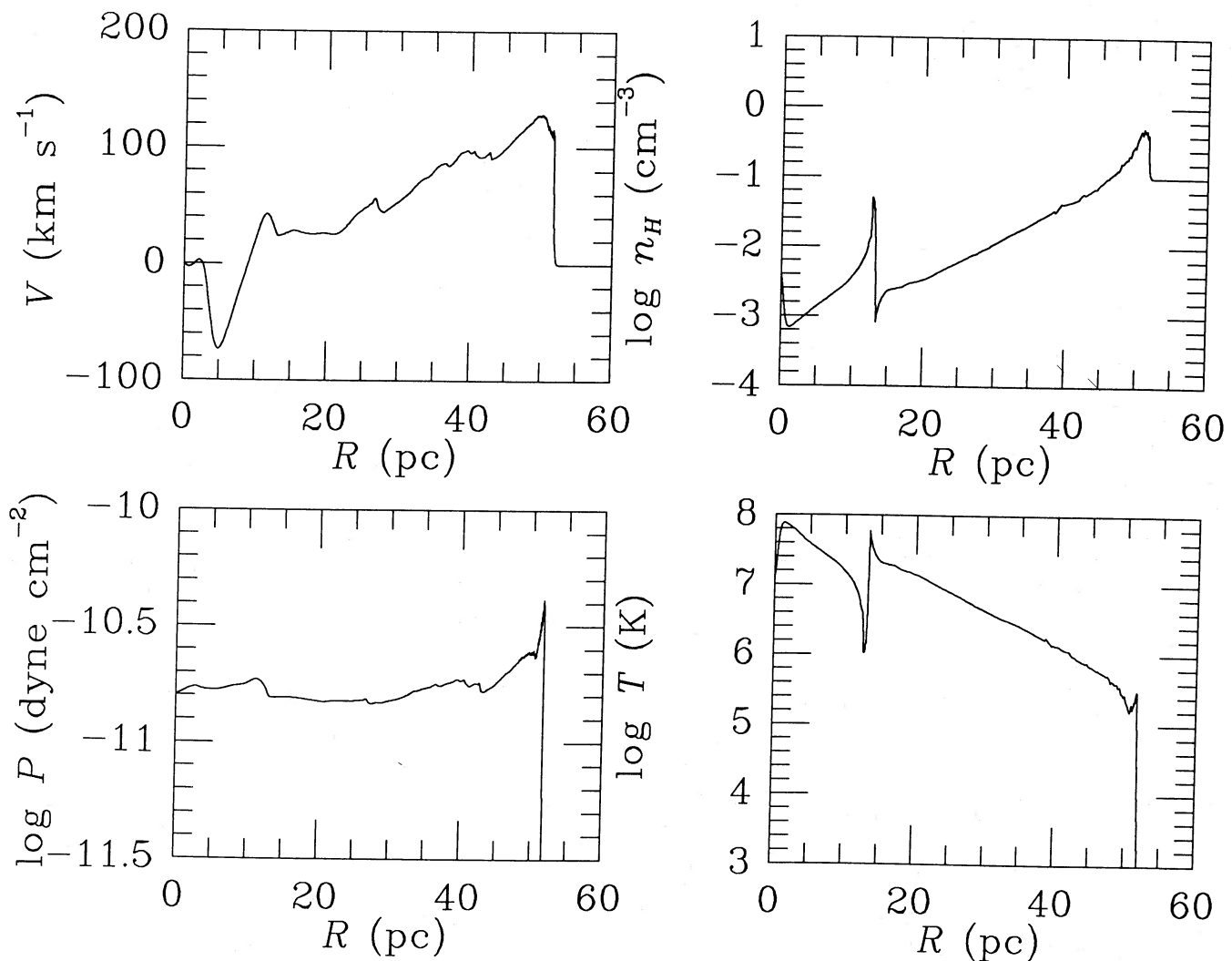
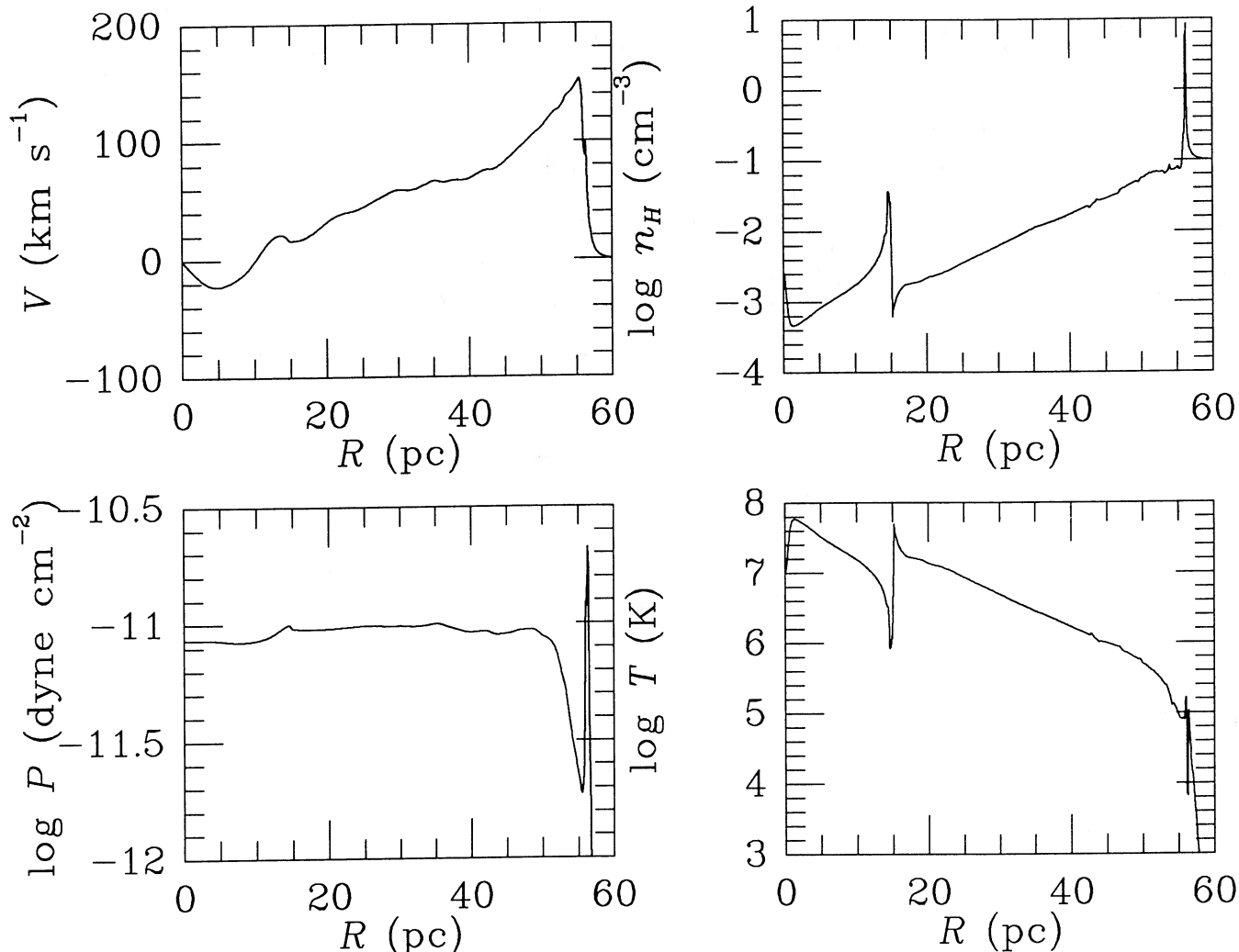


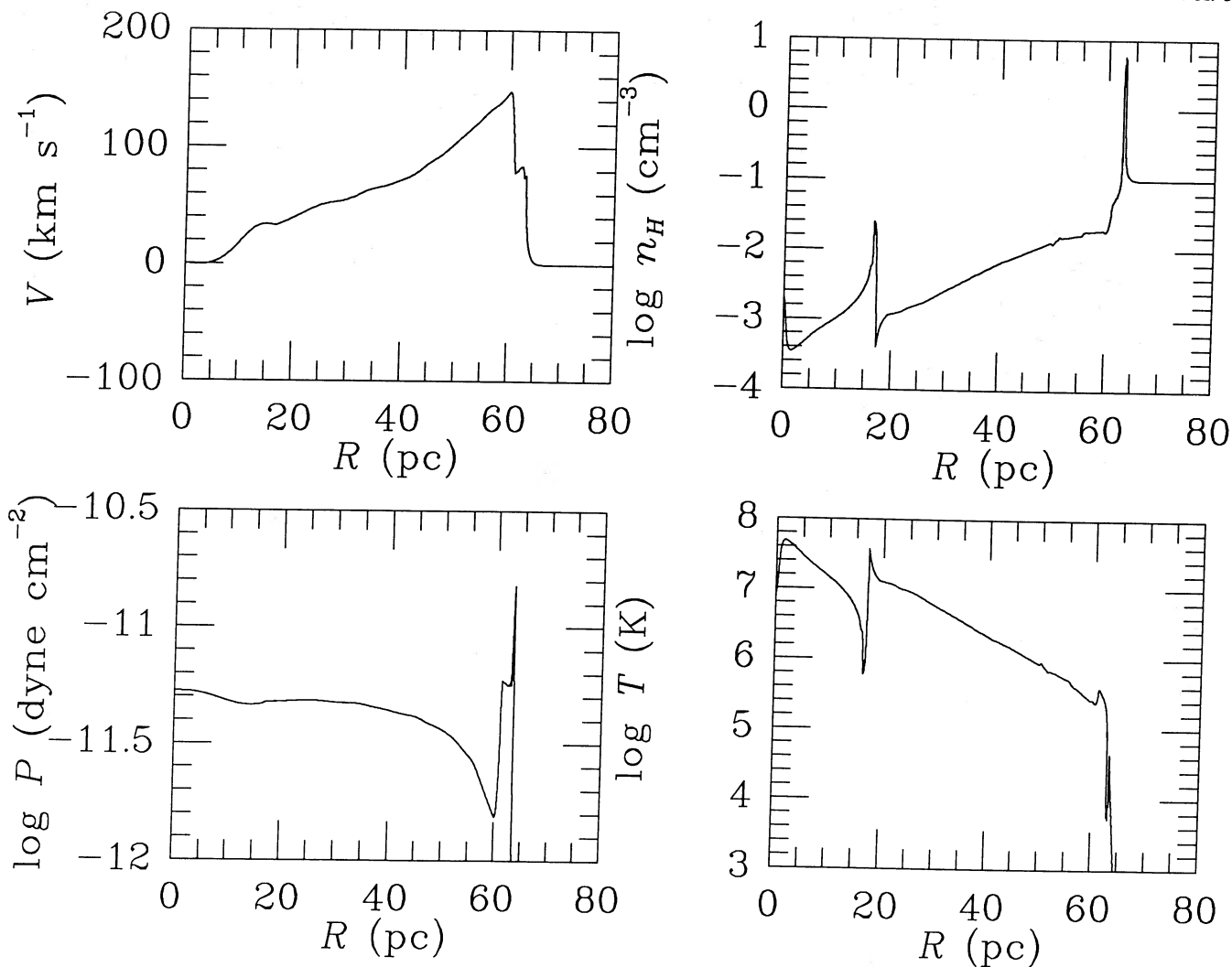
FIG. 1.—The structure of a spherical supernova remnant calculated using a high-resolution numerical hydrodynamics code. The remnant age is  $t = 1.2 \times 10^5$  yr.

FIG. 2.—Same as Fig. 1, for  $t = 1.7 \times 10^5$  yr

radiation. Several interesting features may be noticed. First, the ejecta lie interior to 13 pc and are separated from the interstellar medium by a contact discontinuity with roughly the same density jump as in the initial conditions. In a real supernova remnant this sharp boundary would be destroyed because it is subject to a Rayleigh-Taylor instability during the initial ejecta stage, with the ejecta then being mixed throughout the supernova interior (Gull 1973). A spherically symmetric simulation prevents this instability from occurring. Second, Figure 1 shows many wiggles present in the fluid distributions, particularly in the velocity and pressure profiles. These wiggles are all real and are due to sound waves and weak shock waves. Simulations with half and twice the density of grid points show precisely the same features. A careful examination of these waves shows that they originate from the reflection of the initial reverse shock at the origin. The reflected shock travels back through the ejecta and is partially reflected and partially transmitted at the contact discontinuity. Reflected weak shock waves travel repeatedly back and forth through the ejecta before the acoustic energy is dissipated into heat or transmitted into the interstellar gas. In a realistic three-dimensional model these echoes of "thunder" would reverberate from dense ejecta fragments and interstellar inhomogeneities. The

amplitude of the acoustic waves would be diminished in three dimensions because of the addition of nonspherical modes and because of the absence of a well-defined contact discontinuity, but the total acoustic energy should remain about the same as in our simulation. The generation of sound waves from scattering of a shock by density inhomogeneities was predicted by Spitzer (1982) and studied numerically by Ikeuchi and Spitzer (1984).

Because the postshock flow is subsonic, acoustic waves generated in the interior of the remnant must eventually catch up with the blast wave. In the present simulation the first weak shock wave transmitted at the contact discontinuity catches up with the outer shock at  $t = 1.1 \times 10^5$  yr. The close agreement of this time with the beginning of the radiative stage is a coincidence since a higher interstellar density would lead to cooling before sound waves reach the blast wave. The fact that the radiative stage begins after less than one sound-crossing time for typical ejecta masses and interstellar densities implies that the supernova remnant never completely relaxes to the ST adiabatic similarity solution. This is clearly shown by the velocity and pressure profiles of Figure 1 and will be confirmed by the shock propagation law presented later. Chevalier (1974) did not discover this effect because his initial explosion energy

FIG. 3.—Same as Fig. 1, for  $t = 2.5 \times 10^5$  yr

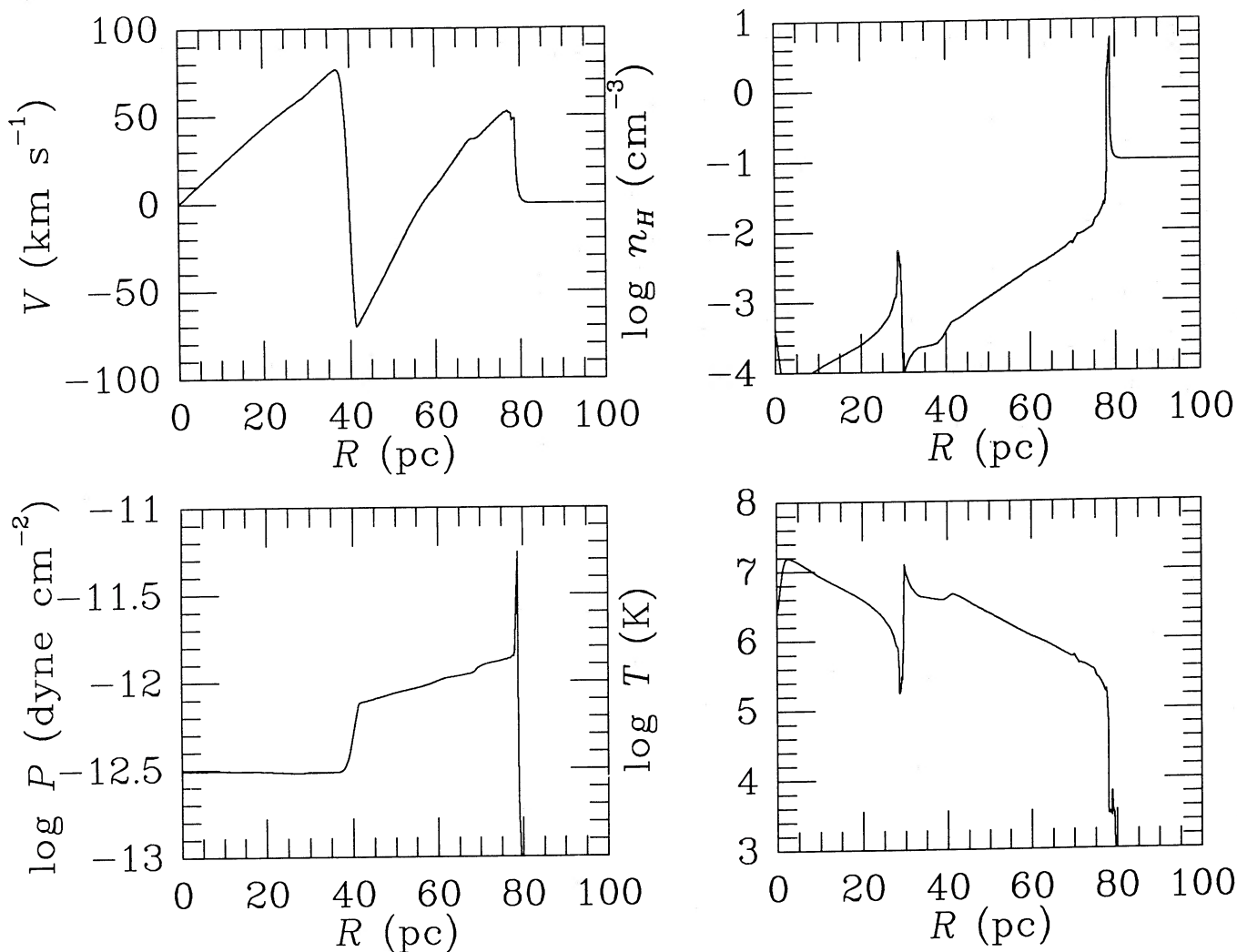
was deposited as heat in a small volume so that the ST solution was quickly, albeit unphysically, established. Mansfield and Salpeter (1974) began with rapidly expanding cold ejecta and their simulations show the non-self-similar behavior, although with less resolution than the present work.

After postshock cooling becomes important the postshock pressure and temperature quickly plummet to low values (Straka 1974)—in the present case the temperature falls to  $T_c = 1.2 \times 10^4$  K before radiative cooling is cut off. The pressure drop causes matter to be driven into the dense cooling region from the interior. A complicated series of shocks, rarefaction waves, and contact discontinuities is formed on subparsec scales inside the shell. The details of this structure are interesting, but the present hydrodynamical simulation does not give correctly the detailed structure in the shell because of the simplified cooling law used. The present results do strongly suggest, however, that time-dependent effects are important in the formation of the radiative shell. Using realistic ionization, radiative transfer, and cooling, Innes *et al.* (1987) also conclude that the evolution of a radiative shock is far from being steady.

Figure 2 shows the remnant structure at  $t = 1.7 \times 10^5$  yr, when the density in the shell reaches a maximum (for the

cooling law used here). The peak density,  $n \approx 10$  cm<sup>-3</sup>, agrees approximately with the density increase  $\mu v_s^2/kT_c$  expected for a steady radiative shock (Spitzer 1978); the agreement is not perfect because the flow inside the shell is unsteady. Interior gas continues to cool and accrete onto the back of the shell so that the interior mass and density drop. The interior pressure is nearly uniform because most of the acoustic energy has been damped or transmitted to the radiative shell. The shell does not reflect sound waves back into the interior because the interior gas is flowing toward the shell supersonically. Thus, gas accretes onto the back of the shell through a shock wave, where the rapidly moving interior gas is decelerated to the common velocity of the shell and outer blast wave (Gaffet 1983). Initially this inner shock is radiative.

Figure 3 shows the remnant structure at  $t = 2.5 \times 10^5$  yr. Beginning at this time the cooling cutoff temperature is gradually decreased ( $T_c \propto t^{-1.4}$ ) so that the relative shell thickness remains roughly constant hereafter; this prevents the computational difficulties which arise from too-thin shells (time step too small) or too-thick shells (loss of interior resolution). The temperature of the gas in the shell actually drops below  $T_c$  because of adiabatic expansion cooling. The accretion shock on the interior of the shell is now clearly visible, 2 pc behind the outer

FIG. 4.—Same as Fig. 1, for  $t = 5.0 \times 10^5$  yr

blast wave, as a discontinuity in the fluid variables. As interior gas of progressively lower density passes through this inner shock, cooling becomes less important and the shock becomes adiabatic. Consequently, the shocked interior gas is not strongly compressed and the accretion shock begins to separate from the shell. After this time the inner shock has little effect on the shell dynamics except to maintain a pressure force on the shell by transforming the ram pressure of interior gas into thermal pressure. At first the inner shock moves outward in Eulerian radius but eventually it reverses to travel back through the cavity in a pattern familiar from the early ejecta stage. Chevalier (1974) found the same effect, although his simulations had much less resolution. We see that the hydrodynamics of supernova remnant evolution is rich with complications, which can be understood when revealed by numerical simulations.

At the last time shown,  $t = 5.0 \times 10^5$  yr in Figure 4, the inner shock has nearly reached the ejecta. Although the velocity jump across this shock is fairly large ( $150 \text{ km s}^{-1}$ ), the interior is still hot so that the shock is weak (Mach number 1.5). After the shock strikes the ejecta, a series of reflected and transmitted weak shocks is again formed as waves travel repeatedly through the ejecta and through the SNR cavity. These waves are now reflected at the shell because the interior

is fully subsonic; the echoes persist through the end of the simulation at  $1.75 \times 10^6$  yr.

### III. ANALYTIC MODELS

In this section we develop analytic models for the dynamics of SNR expansion. Understanding the dynamics leads to precise kinematics, a prerequisite for accurate luminosity. We explain how radiative cooling and a nonlinear distribution of material within the remnant obviates the standard kinematical power-law approximations. First we derive an ordinary differential equation (ODE) which expresses Newton's second law for the blast wave, and integrate it. We next simplify the ODE and solve the system analytically with moderate accuracy, as compared to the numerical solution, over a broad time interval. Cox's (1972) analytic model, with improved cooling, is found to give a good approximation for  $v(R_s)$  over a shorter time interval. Last, we present an approximate offset power-law analytic solution for the PDS stage. Following this section, we shall use these analytic solutions to examine the late-time behavior of an SNR.

A striking feature of the numerically simulated SNR evolution in § II is the continual variation of the logarithmic derivative  $d \ln R_s / d \ln t = v_s t / R_s$  (see Fig. 5). This quantity is

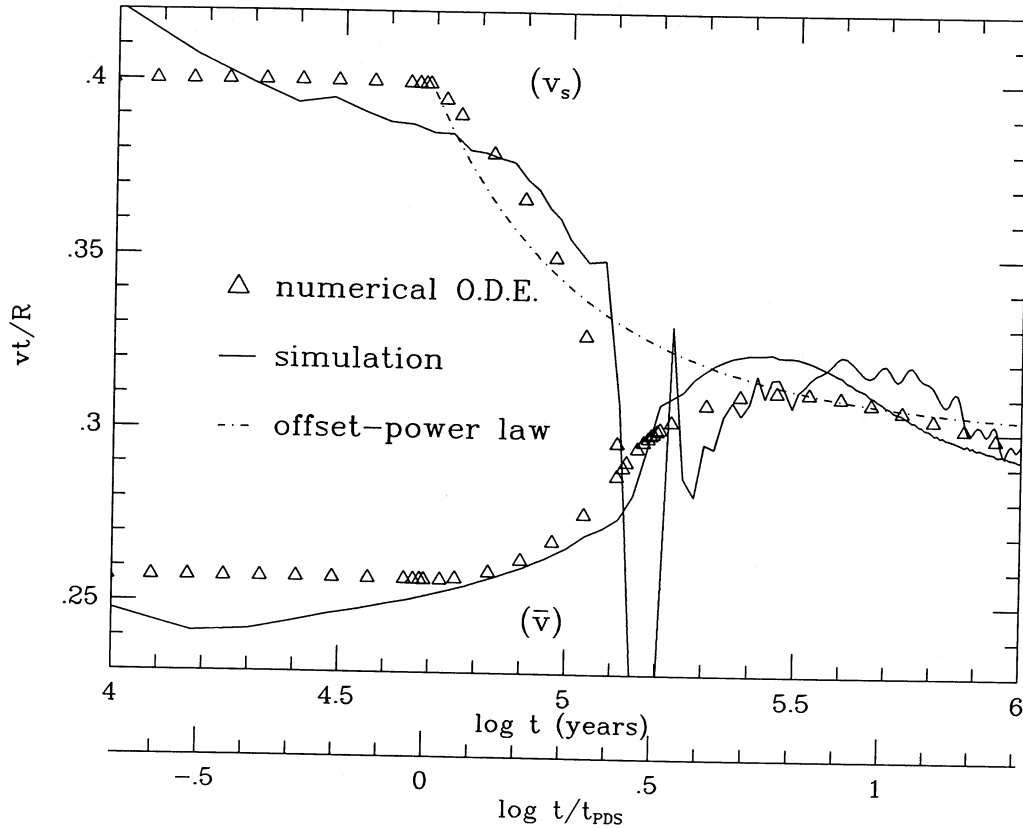


FIG. 5.—The dimensionless ratios  $v_s t/R_s$  and  $\bar{v} t/R_s$  vs. time. Both quantities are shown from the hydrodynamical simulation (solid lines) and from the numerical solution to the ordinary differential eq. (3.17) (triangles); the lower curves portray the mass-averaged ratio  $\bar{v} t/R_s$ , and the upper curves use the shock velocity,  $v_s t/R_s$ . From the offset power-law solution (3.32),  $v_s t/R_s$  is plotted. The uneven spacing of the triangles results because the integrating software automatically chooses narrower steps at the transitional times  $t_{\text{PDS}}$  and  $t_{\text{sf}}$ .

constant for self-similar blast waves and standard power-law solutions of the form  $R = At^\eta$ , with  $A$  constant. These standard solutions, however, apply only under narrow conditions which radiating SNRs cannot meet. In particular, they require two unphysical events: a drop in the mean interior pressure at the PDS onset, and subsequently negligible radiative cooling of the interior. In addition, if the evolution of the SNR is divided into several stages, with the  $i$ th stage lasting from time  $t_i$  to  $t_{i+1}$ , then the standard solutions will exhibit discontinuities in  $d \ln R/d \ln t$  at the beginning of each stage; i.e., as we shall show below, one cannot ignore constants of integration.

We demonstrate these difficulties by examining the following simplified system in which we approximate the evolving SNR as a sphere containing all the mass in a thin shell at the edge ( $R_s$ ), moving at the postshock fluid velocity. We then set the total change in momentum of the SNR equal to the force exerted by the mean pressure on the interior wall:

$$\frac{d}{dt} (M_s v_1 v_s) \simeq 4\pi R_s^2 \bar{P}, \quad (3.1)$$

where  $M_s = 4/3\pi R_s^3 \rho_0$  is the mass of the SNR,  $\rho_0$  is the ambient mass density, and  $\bar{P}$  is the average interior pressure. The fluid velocity behind the shock is  $v_1 v_s$ , where

$$v_1 = \frac{2}{\gamma + 1} \quad (3.2)$$

is constant both in the limit of negligible radiation and in the limit that radiation is so strong that the effective  $\gamma$  is unity. We

also write

$$\bar{P} \equiv \frac{\rho_0 v_s^2}{\alpha^2}, \quad (3.3)$$

where  $\alpha$  is the shock's effective mean Mach number relative to the interior gas (McKee and Ostriker 1977).

Equation (3.1) admits power-law solutions provided that

$$\alpha^2 v_1 = \frac{3\eta}{4\eta - 1}. \quad (3.4)$$

Under the assumption that  $\alpha^2$  is constant (i.e., the blast wave is self-similar), equation (3.3) and the power-law assumption together imply that  $\bar{P} \propto R_s^{-k_p}$ , which yields

$$\eta = \frac{2}{2 + k_p}, \quad (3.5)$$

where the physical conditions of the interior determine the constant  $k_p$ .

In the Sedov-Taylor stage the interior loses no energy and the system does no work on the external medium; the pressure, being proportional to the energy density, decreases solely because of the increased volume, so that  $k_p = 3$  and  $\eta = \frac{2}{5}$ . In the PDS stage (with no interior cooling), the interior loses energy because it pushes the shell into the ISM. This configuration is analogous to a reversible, adiabatic system, where  $PV^\gamma$  is constant ( $V$  is the volume). When  $\gamma = 5/3$ ,  $k_p = 5$  and  $\eta_{\text{PDS}} = \frac{2}{7}$ . These standard values of  $\eta$  now constrain  $\alpha^2 v_1$  to 2

and 6 for the ST and PDS stages, respectively; since we know from the strong-shock approximation that  $v_{1(\text{ST})} = \frac{3}{4}$  and  $v_{1(\text{PDS})} = 1$ ,  $\alpha_{\text{ST}}^2$  must equal 8/3 and  $\alpha_{\text{PDS}}^2$  must be 6 for these solutions to be viable. (When calculated from the exact interior ST solution, not a zero-thickness shell,  $\alpha_{\text{ST}}^2 = 2.840$  [Ostriker and McKee 1988], which is closer to  $20/7 = 2.857$  than  $8/3 = 2.667$ .) Of course, with no interior pressure  $\alpha_{\text{MCS}} \rightarrow \infty$  and  $\eta_{\text{MCS}} = \frac{1}{4}$  from equation (3.4) alone.

Despite the simplifications employed, this exercise demonstrates that the standard power-law solutions exist only for specific, constant values of the mean Mach number  $\alpha$  and the product  $\alpha^2 v_1$ . At the transition to the PDS stage the remnant is overpressured with respect to the standard  $\frac{2}{7}$  law, which requires  $\alpha^2 = 6$ . Thus the effective value of  $\eta_{\text{PDS}}$  may exceed  $\frac{2}{7}$ . In a similar manner the existing interior pressure greatly delays the appearance of any momentum-conserving snowplow, even allowing for cooling of the interior.

#### a) Blast Wave Equation of Motion

The abrupt restructuring of the remnant at the formation of the shell necessitates a more sophisticated treatment of the dynamics during the transition from the ST to the PDS stage. Because the shock velocity  $v_s$  rapidly changes during the transition, we consider the mass-averaged quantity,  $R_s^3 \bar{v}$ , which varies smoothly. Replacing equation (3.1) by the physically exact equation of motion for a blast wave (Ostriker and McKee 1988), we have

$$\frac{d}{dt} (M_s \bar{v}) = 4\pi R_s^2 K_P \bar{P}, \quad (3.6)$$

where

$$K_P \equiv 2 \int_0^{R_s} \frac{P(r)}{\bar{P}} \frac{r}{R_s} \frac{dr}{R_s} \quad (3.7)$$

is of order unity; for an ST blast wave with  $\gamma = 5/3$ ,  $K_P = 0.918$ , whereas for an isobaric blast wave  $K_P = 1$ . The mean velocity is

$$\bar{v} \equiv K_{01} v_1 v_s, \quad (3.8)$$

where, in general, in terms of an integration through mass  $m$ , one has

$$K_{ij} \equiv \int_0^{M_s} \left[ \frac{r(m)}{R_s} \right]^i \left[ \frac{v(m)}{v_1 v_s} \right]^j \frac{dm}{M_s}. \quad (3.9)$$

The moments  $K_{ij}$  are constant for self-similar blast-waves. As with  $K_P$ , they are generally close to unity, and as  $\gamma$  approaches unity the moments do also. For an ST blast wave with  $\gamma = 5/3$ , Ostriker and McKee (1988) find  $K_{01} = 0.857$ .

The transition from the ST to the PDS stage occurs near the shell-formation time  $t_{\text{sf}}$ , when the first element of gas cools to zero temperature. For our analytic work we use a cooling function proportional to  $T^{-1/2}$ , appropriate for collisionally ionized gas at temperatures  $10^5 \text{ K} \lesssim T \lesssim 10^{7.5} \text{ K}$ :  $\Lambda = 1.6 \times 10^{-19} \zeta_m T^{-1/2} \text{ ergs cm}^3 \text{ s}^{-1}$ , where the metallicity factor  $\zeta_m = 1$  for solar abundances (e.g., McKee 1982). The shell formation time is then

$$t_{\text{sf}} = 3.61 \times 10^4 \frac{E_{51}^{3/14}}{\zeta_m^{5/14} n_0^{4/7}} \text{ yr}, \quad (3.10)$$

where  $n_0$  is the ambient hydrogen density in units of  $1 \text{ cm}^{-3}$ ,  $E_{51}$  is the initial SNR energy in units of  $10^{51} \text{ erg}$  (Cioffi and

McKee 1988; similar estimates, using slightly different methods, have been given by Cox 1972, 1986; and Cox and Anderson 1982). As one might expect, however, radiative losses affect the evolution before  $t_{\text{sf}}$ , so we somewhat arbitrarily adopt

$$t_{\text{PDS}} \equiv \frac{t_{\text{sf}}}{e}, \quad (3.11)$$

where  $e$  is the base of the natural logarithm, as the end of the ST stage and the beginning of the PDS stage. Note that equation (3.10) yields a shell-formation time in good agreement with the numerical simulation,  $1.3 \times 10^5 \text{ yr}$ ; see Figure 5.

We can obtain an accurate approximation to the solution for the equation of motion of the blast wave by noting that  $v_1$ ,  $K_P$ , and  $K_{01}$  are all known and close to unity in the ST stage ( $t < t_{\text{PDS}}$ ), and they approach unity for  $t \gg t_{\text{sf}}$ . We treat the transition from the ST to the PDS stage as being a smooth change in  $\gamma$ , or equivalently,  $v_1$  (eq. [3.2]), as the interior mass and velocity distributions slowly evolve from the ST, adiabatic form to the radiative form. Using Ostriker and McKee's (1988) "pressure gradient approximation" (which for  $\gamma = 5/3$  is equivalent to Gaffet's [1978] approximation in which the pressure is a linear function of mass), we find

$$K_{01}(v_1) = \frac{6}{(7 - 4v_1)(1 + v_1)}, \quad (3.12a)$$

$$K_P(v_1) = \frac{3(9 + v_1 - 4v_1^2)}{(7 - 4v_1)(1 + v_1)(5 - 2v_1)}. \quad (3.12b)$$

We completely specify the moments by adopting an *Ansatz* for  $v_1$ : we know that  $v_1 = \frac{3}{4}$  in the ST stage ( $t \leq t_{\text{PDS}}$ ), and the details of the cooling calculation (Cioffi and McKee 1988) suggest trying

$$v_1 = \frac{3}{4} + 0.25 \left( \frac{t_*^{2.1} - 1}{t_{\text{sf}*}^{2.1} - 1} \right) \quad (3.13)$$

for  $t_{\text{PDS}} \leq t \leq t_{\text{sf}}$ , where  $t_* \equiv t/t_{\text{PDS}}$ ,  $t_{\text{sf}*} \equiv e$ , and, in general, the asterisk subscript denotes that a quantity  $x$  has been normalized to its (analytic) value at the end of the ST stage,  $x_{\text{PDS}}$ :

$$x_* \equiv \frac{x}{x_{\text{PDS}}}. \quad (3.14)$$

At late times ( $t_* \gg 1$ ),  $v_1$  approaches its maximum value. If the cooling were total, with an infinitesimally thin radiative shell, then this maximum value would be unity. Although in our numerical simulation the shell has a finite thickness because the cooling ceased below  $T_c \leq 1.2 \times 10^4 \text{ K}$ , small deviations from  $v_1 = 1$  after  $t_{\text{sf}}$  do not significantly improve our agreement with the hydrodynamical simulation. We therefore prefer the simplicity of  $v_1 = 1$  for  $t \geq t_{\text{sf}}$ .

We next need a better estimate of the mean pressure,  $\bar{P}$ . Although the interior in our hydrodynamical simulation never relaxes completely to the Sedov-Taylor similarity solution, the standard ST radius (eq. [3.31]) and velocity values agree with those from the simulation to  $\lesssim 1\%$  and  $\lesssim 3\%$ , respectively. This agreement suggests that the overall adiabatic approximation works well, though the remnant in fact cools continuously and has radiated away some small fraction ( $\approx 2\%$ ) of the original energy by the time we choose to end this second stage. When we calculate the cooling in the PDS stage (Cioffi and McKee 1988), we find that the thermal energy  $E_{\text{th}}$  varies as

$t^{-4/9}$  in addition to the usual radial dependence noted above ( $E_{\text{th}} \propto R^{-2}$ ). We therefore combine two terms, one embodying the adiabatic temporal dependence and the other the post-shell formation dependences, giving us a form for the energy which is smooth from early to late times:

$$\frac{E_{\text{th}}}{E_{\text{th(ST)}}} = a_1 \left[ 1 - \left( \frac{t}{a_2 t_{\text{sf}}} \right)^{14/5} \right] \times H(a_2 t_{\text{sf}} - t) + \frac{1 - a_1}{\left[ \left( \frac{R_s}{R_{\text{sf}}} \right)^{10} + 1 \right]^{1/5} \left[ \left( \frac{t}{t_{\text{sf}}} \right)^4 + 1 \right]^{1/9}}, \quad (3.15)$$

where  $a_2 t_{\text{sf}}$  is the time at which all the interior thermal energy would be radiated away if the remnant remained in the Sedov-Taylor stage, the step function  $H(t) = 1$  if the argument is positive, and zero otherwise, and we have normalized to the energy of the analytic Sedov-Taylor solution,  $E_{\text{th(ST)}} = 0.717 E$  (e.g., Ostriker and McKee 1988). For the shell-formation time ( $t_{\text{sf}}$ ) and the radius at that time ( $R_{\text{sf}}$ ), we use the analytic results, equations (3.10), (3.11), and (3.31). We fitted the simulation interior thermal energy versus time to adjust the two constants, finding  $a_1 = 0.398$  and  $a_2 = 1.169$ . Figure 6 shows the fit; at  $\log t_* \simeq 0.5$  the ST contribution has been eliminated. We use this energy evolution to determine the mean pressure

$$\bar{P} = \frac{E_{\text{th}}}{2\pi R_s^3}; \quad (3.16a)$$

at late times ( $t_* \gg 1$ ), we have for the normalized pressure

$$\bar{P}_* \equiv \frac{\bar{P}}{\bar{P}_{\text{PDS}}} \equiv \frac{\bar{P}}{[E_{\text{th(ST)}}/2\pi R_{\text{PDS}}^3]} \rightarrow \frac{1.92}{R_*^5 t_*^{4/9}}, \quad (3.16b)$$

where we have dropped the subscript  $s$  in the normalized radius,  $R_* \equiv R_s/R_{\text{PDS}}$ .

We now have expressions for all relevant terms in equations (3.6) and (3.8). By using the variables  $R_s^3 \bar{v}$  and  $R_s^4$ , no time derivatives of the moments are needed, so the blast wave is governed by the following system of coupled ordinary differential equations:

$$\frac{d}{dt_*} (R_*^3 \bar{v}_*) = \frac{3}{5} \frac{K_P}{K_{P(\text{ST})}} \bar{P}_* (R_*^4)^{1/2} \quad (3.17a)$$

$$\frac{d}{dt_*} (R_*^4) = \frac{8}{5} \frac{K_{01(\text{ST})}}{K_{01}} \frac{v_{1(\text{ST})}}{v_1} (R_*^4 \bar{v}_*), \quad (3.17b)$$

where  $\bar{v}_* \equiv \bar{v}/\bar{v}_{\text{PDS}}$ . The mean fluid velocity at the onset of the PDS stage  $\bar{v}_{\text{PDS}}$  is taken to be that at the end of a self-similar ST stage,

$$\bar{v}_{\text{PDS}} \equiv K_{01(\text{ST})} v_{1(\text{ST})} v_{\text{PDS}} \quad (3.18)$$

from equation (3.8); for  $\gamma = 5/3$ , we have  $\bar{v}_{\text{PDS}} = 0.643 v_{\text{PDS}}$ . In deriving equation (3.17) we have also used the relation  $K_{P(\text{ST})}/(K_{01(\text{ST})} v_{1(\text{ST})} \alpha_{\text{ST}}^2) = \frac{1}{2}$  (Ostriker and McKee 1988, eq. [D.9]). Note that equations (3.17a) and (3.17b) are *exact*; the approximations enter in determining  $K_P$ ,  $K_{01}$ ,  $v_1$ , and  $\bar{P}_*$ .

We attempted many other forms of these basic equations, but only this specific set produced such good results. We

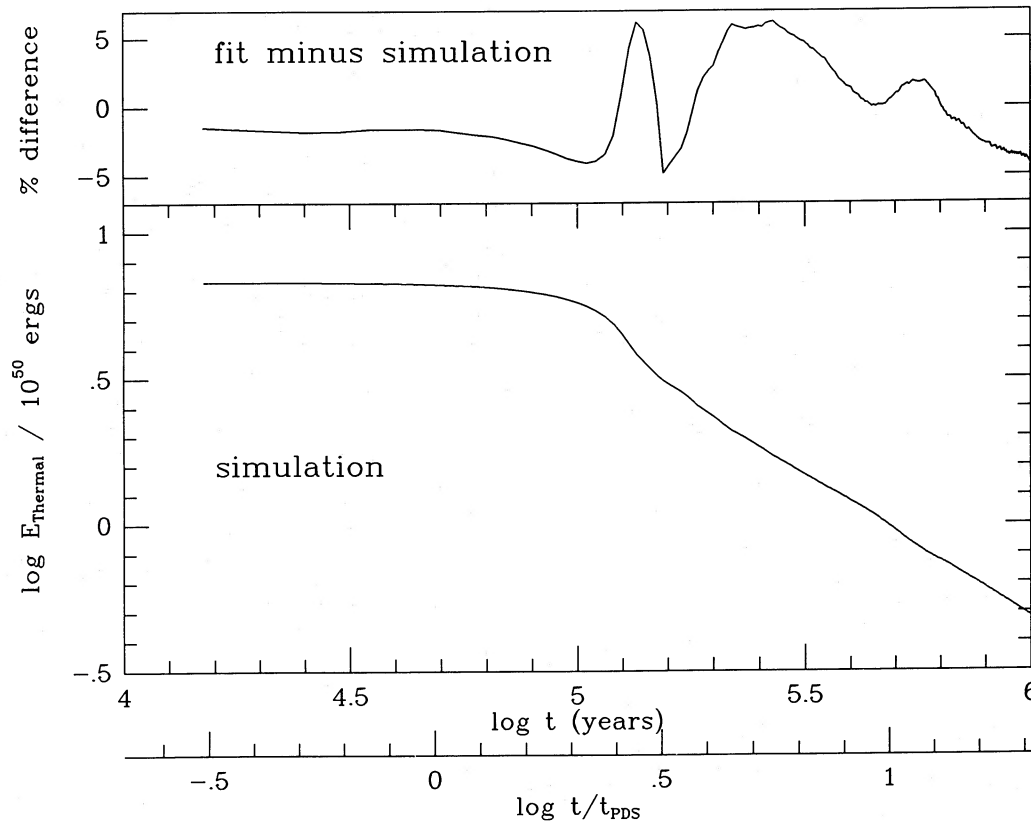


FIG. 6.—The thermal energy of the interior, vs. time, from the hydrodynamical simulation. The upper curve shows the percentage difference between our analytic fit (eq. [3.15]) and the simulation, against the same abscissa.

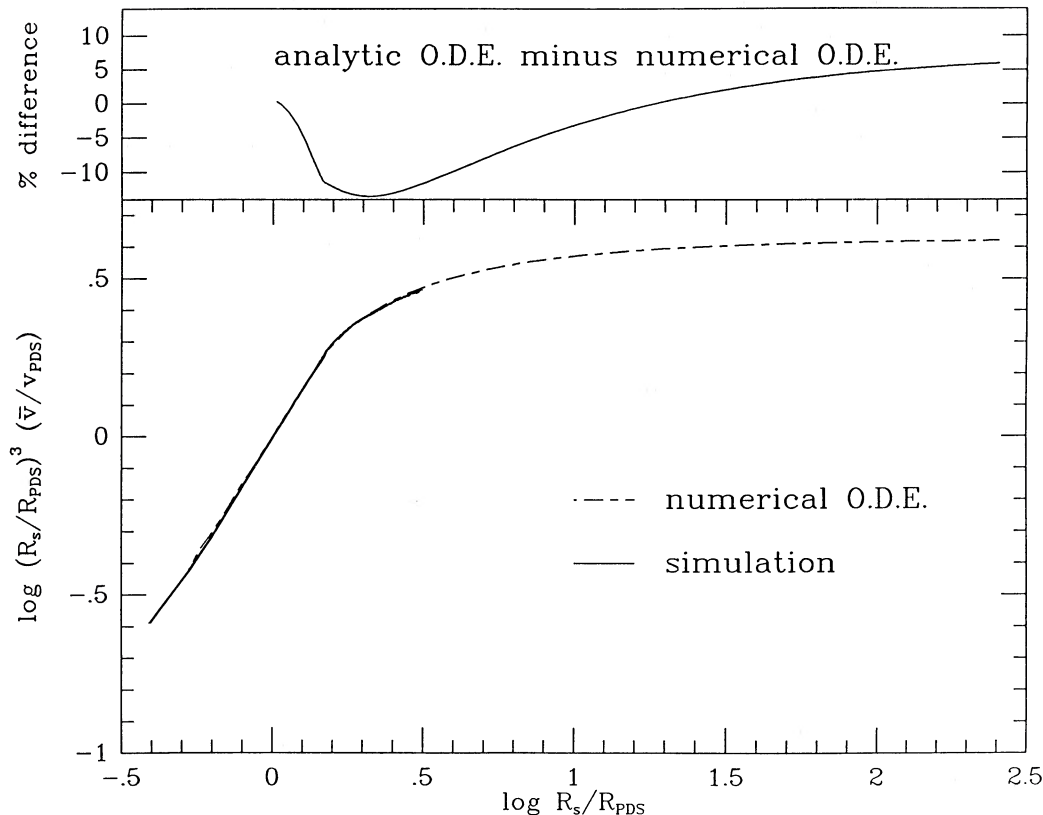


FIG. 7.—The late-time behavior of SNR expansion as exemplified by the momentum from the hydrodynamical simulation and the numerical solution to the system of ordinary differential eqs. (3.17). We normalize the momentum to the value at the PDS onset. The upper curve shows the percentage difference between the analytic and numerical solutions to the differential equations. Transition to the MCS stage or merger with the ISM has been neglected. The solution has been extended to unphysically late times (even exceeding the Hubble time) in order to demonstrate graphically the slow convergence of the momentum to its final value.

solved the equations numerically, and in Figure 7 plot the momentum from the ODE and from the hydrodynamical simulation against the radius, both normalized to their values at the PDS onset. The numerical ODE solution stays just slightly above ( $\lesssim 5\%$ ) the simulation, but when one considers the approximations and that our fit to the pressure (eqs. [3.15] and [3.16]) is the only tie to the simulation, this remarkable agreement underscores the validity of our dynamical approach: we can reproduce a basic physical characteristic of an evolving SNR, its momentum.

On the other hand, the progression of the logarithmic derivative provides a detailed view of the kinematical behavior, as it easily shows small changes in the effective power-law index  $vt/R_s$ . Figure 5 shows this index from the hydrodynamical simulation and from the solution of the system (3.17). We can form this quantity using either the shock velocity  $v_s$  or the mass-averaged velocity  $\bar{v}$ , and we show both on Figure 5. The ODE matches the simulation well, especially in duplicating the rise near the shell-formation time as the “overpressured” interior pushes on the shell. With this excellent agreement between our hydrodynamical simulation and the solution to our blast-wave equation of motion, we argue that our model accurately represents the dynamical evolution of an idealized supernova remnant. We exploit this enhanced understanding in the analytic approaches which follow.

#### b) Analytic Solutions to the Blast-Wave Differential Equation

Here we attempt to reconstruct analytically the numerically determined behavior of the previous section by solving a sim-

plified equation of motion (3.6). We write the pressure as a power law, and, where necessary, we replace slowly varying coefficients by their asymptotic values. We can approximate the force on the shell (i.e., the right-hand side of eq. [3.6]) by a power law in time or radius. In either case the first integration of the ordinary differential equation finds the momentum of the remnant, proportional to  $R_s^3 \bar{v}$ . Comparison of this quantity with the momentum from the numerical solution directly tests the accuracy of this analytic technique, especially at late times as the SNR evolves to a momentum-conserving snowplow.

Cox (1972), who assumed no interior radiative cooling (i.e., he neglected the  $t_*^{4/9}$  dependence in eq. [3.15]), found a solution with the velocity expressed as a function of radius. He calculated a cooling time and extended the Sedov-Taylor solution to find the radius and velocity at that time. Since the cold shell slows to the velocity of the fluid behind the shock, the ST shock velocity would be too high for the PDS stage. Instead of the analytic factor of the postshock fluid velocity equaling 0.75 of the shock velocity in the adiabatic stage, Cox used 0.6 of the ST shock velocity. We revised his solution only by using a more modern cooling law, as written in this paper, and produced

$$v_*^2 = \frac{2.03}{R_*^5} \left( 1 - \frac{0.75}{R_*} \right). \quad (3.19)$$

As we show in Figure 8, this solution matches well the hydrodynamical simulation after shell formation. With a radial power law for the force in our blast-wave equation (3.6), we

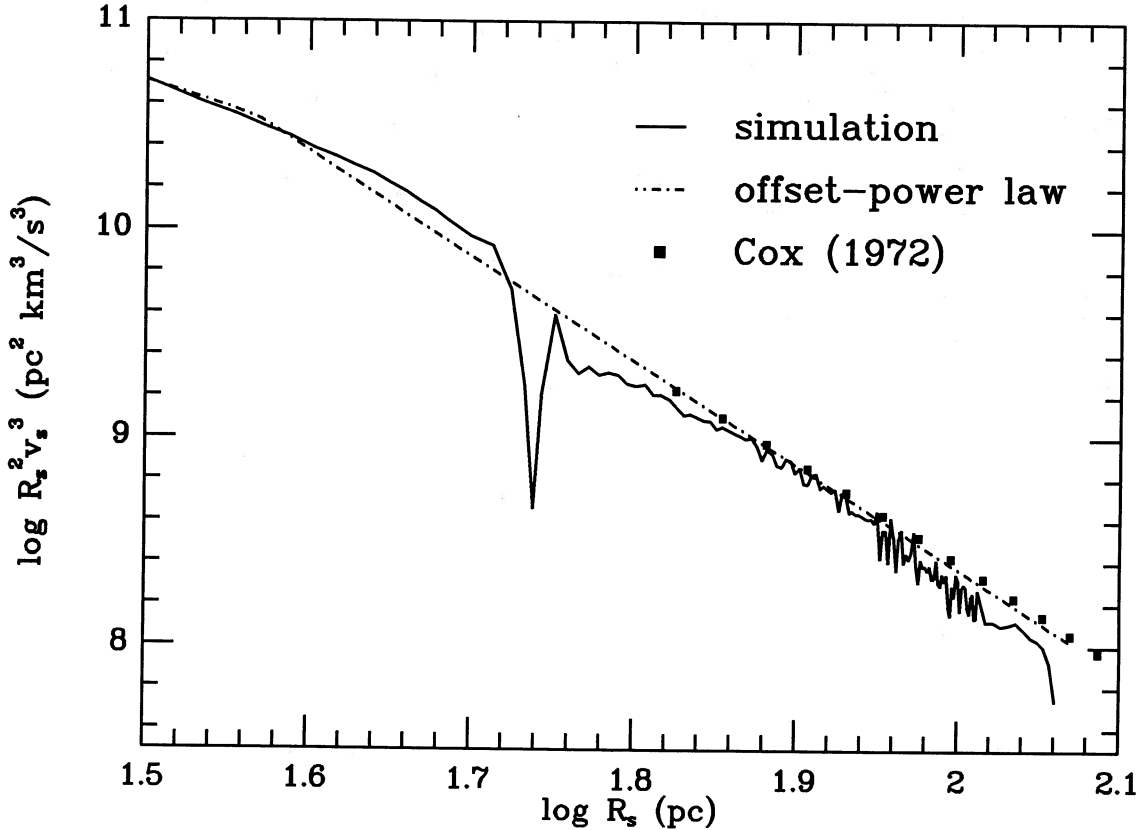


FIG. 8.—The product  $R_*^2 v_*^3$  vs. time, from the hydrodynamical simulation and the offset power-law formulae (eqs. [3.32] and [3.33]). Once the shock is fully radiative, the luminosity is proportional to  $R_*^2 v_*^3$ . Cox's (1972) result for this quantity (based on eq. [3.19]) is also shown. For this case,  $R_{\text{PDS}} = 36.8 \text{ pc} = 10^{1.57} \text{ pc}$ .

obtain the velocity as a function of radius. If we make the same approximations as Cox, we can reproduce his  $v(R)$  solution. However, Cox did not intend this solution for very late times, where it would establish a pressure-driven snowplow expansion with  $R_s \propto t^{2/7}$  rather than the momentum-conserving  $R_s \propto t^{1/4}$ ; it is within 15% of the numerical simulation for  $1.6 \lesssim R_* \lesssim 3$ , or  $5 \lesssim t_* \lesssim 35$ . If we retain interior cooling, our solution does evolve to an MCS stage. We find, however, that when the force is expressed as a temporal rather than a radial power law, we obtain a more accurate solution. In the following, we explicitly develop this calculation as a function of time only.

At late times the evolution of the SNR depends only weakly on the pressure, whereas the much larger pressure at the PDS onset strongly influences the future evolution of the remnant. Therefore, we choose to require the correct value of  $\bar{P}$  at  $t_* = 1$  rather than as  $t_* \rightarrow \infty$ , and we approximate the force by the following power law in time:

$$4\pi R_s^2 K_P \bar{P} = 4\pi R_{\text{PDS}}^2 K_{P(\text{ST})} \bar{P}_{\text{PDS}} t_*^{-q}. \quad (3.20)$$

Asymptotically, when  $t \gg t_{\text{PDS}}$  we have

$$q \rightarrow 3\eta + \frac{4}{3}, \quad (3.21)$$

from equations (3.15) and (3.16), and, as  $\eta \rightarrow \frac{1}{4}$ ,  $q \rightarrow 43/36$ . Because  $q \approx 1$ , the momentum of the shell converges slowly to its final value. A first integration of equation (3.6) (or, equivalently, eq. [3.17a]) to any normalized time  $t_*$  from  $t_* = 1$  yields

$$R_*^3 \bar{v}_* \simeq 1 + \frac{3}{5} \left( \frac{1 - t_*^{-q}}{q - 1} \right). \quad (3.22)$$

A second integration, now assuming that the coefficients  $K_{01}$  and  $v_1$  vary sufficiently slowly so that we can remove them from the integral, gives an expression for the radius with two integration constants:

$$R_*^4 \simeq 1 + \frac{24}{25} \frac{K_{01(\text{ST})} v_{1(\text{ST})}}{K_{01} v_1} \times \left[ \frac{5}{3} (t_* - 1) + \frac{(2 - q)t_* - t_*^{2-q} + q - 1}{(2 - q)(q - 1)} \right]. \quad (3.23)$$

For  $t_* \equiv t/t_{\text{PDS}} < 1$ , this yields the ST result  $R_s = R_{\text{PDS}} t_*^{2/5}$ , since then  $R_s^2 \bar{P} \propto R_s^{-1} \propto t^{-2/5}$  so that  $q = \frac{2}{5}$ .

To determine the best  $q$  for times beyond  $t_* = 1$  we use  $K_P = K_{01} = v_1 = 1$ , and we require that the total change in momentum,

$$\int_1^\infty \bar{P} R_*^2 dt_*, \quad (3.24)$$

as determined from our approximate force law (3.20), be identical with that found from integrating the more precise pressure of equations (3.15) and (3.16). We find  $q \approx 1.17$ , only 2% smaller than the asymptotic  $q$  (eq. [3.21]). With this value of  $q$  we have

$$R_*^3 \bar{v}_* \simeq 4.53(1 - 0.779t_*^{-0.17}), \quad (3.25)$$

$$R_*^4 \simeq 4.66t_*(1 - 0.939t_*^{-0.17} + 0.153t_*^{-1}), \quad (3.26)$$

which shows that the momentum slowly converges to a constant, and that correspondingly the solution slowly approaches the momentum-conserving snowplow  $R \propto t^{1/4}$ . Note that at

late times the shock velocity  $v_s$  and the mean velocity  $\bar{v}$  are essentially the same, so that  $v_* = v_s/v_{\text{PDS}} \simeq \bar{v}/v_{\text{PDS}} = 0.643\bar{v}_*$  from equation (3.18).

We compare these results with the numerical solution to the blast-wave ODE. The analytic momentum (3.25) never differs by more than  $\sim 10\%$ , as shown in Figure 7. The radius from (3.26) never differs by more than  $\sim 5\%$ . This analytic ODE solution should therefore accurately represent the extreme late-time behavior of SNR expansion, when  $t \gg t_{\text{PDS}}$ .

### c) Offset Power-Law Solutions for Radiative SNRs

We desire an analytic expression which will reproduce the kinematics of the hydrodynamical simulation to high accuracy and yet be simpler than our ODE solution (3.26). To begin to accomplish this task we must improve upon the unrealistic constant logarithmic derivative seen in the standard power-law solutions. If we relate the velocity and radius by a conventional power law,

$$v_s = v_i \left( \frac{R_s}{R_i} \right)^{-(1-\eta_i)/\eta_i}, \quad (3.27)$$

where  $v_i \equiv v_s(R_i)$ , unlike both our analytic ODE (3.26) and Cox's (1972) solution (3.19), we shall have only one constant of integration in the expression for the radius. Integration of (3.27) gives a power law *offset* in time:

$$R_s \equiv R_i \left[ \frac{(t/t_i) - c_i}{1 - c_i} \right]^{\eta_i}, \quad (t_i \leq t \leq t_{i+1}), \quad (3.28)$$

where  $R_i \equiv R_s(t_i)$ ,  $c_i$  is the integration constant, and in general, the subscript  $i$  denotes the value of a parameter at the beginning of stage  $i$ . With this form of  $R_s(t)$ , the logarithmic derivative approaches  $\eta_i$  asymptotically:

$$\frac{d \ln R_s}{d \ln t} = \eta_i \left( \frac{t}{t - c_i t_i} \right), \quad (3.29)$$

so for  $t_i > t \gg t_{i-1}$  the logarithmic derivative must be  $\eta_{i-1}$ . Although the shock velocity does dip strongly at the formation of the shell (e.g., Fig. 5), the difficulty of calculating the magnitude of the drop, and its short duration, suggests a smooth solution. We make the two values of  $\eta$  continuous by setting

$$c_i = 1 - \frac{\eta_i}{\eta_{i-1}}, \quad (3.30)$$

which is equivalent to requiring that both  $R_s$  and  $v_s$  be continuous across stage boundaries if  $t_{i+1} \gg c_i t_i$ . The constant  $c_i$  thus acts as a normalized offset time which permits continuous solutions and delays the manifestation of the simplest power-law behavior of a constant logarithmic derivative.

We note that Shull (1980) had the radius continuous across the transition to the PDS stage and mentioned that one could avoid his velocity jump by including an arbitrary constant of integration, which Wheeler, Mazurek and Sivaramakrishnan (1980) indeed had done. Cioffi (1985) first used this offset form, which we find both accurate and convenient.

Just prior to the beginning of the pressure-driven snowplow stage we use the standard Sedov-Taylor solution

$$R_s = \left( \frac{\xi E}{\rho_0} \right)^{1/5} t^{2/5}, \quad (3.31)$$

where  $E$  is the initial energy of the explosion, and the numerical

constant  $\xi$  is found to be 2.026 for  $\gamma = 5/3$  (Ostriker and McKee 1988). We use this solution at  $t_{\text{PDS}}$  to obtain  $R_{\text{PDS}}$ . The offset causes the smooth transition from the ST logarithmic derivative of 0.40 to the asymptotic  $\eta_{\text{PDS}}$ . Although  $\eta = \frac{2}{7}$  produces an acceptable solution, we have found that  $\eta_{\text{PDS}} = \frac{3}{10}$  gives better results when directly compared to all points (after  $t_{\text{PDS}}$ ) from our hydrodynamical simulation. This choice reduced the root mean square difference by about a factor of 1.5 in the radius, which changes smoothly across shell formation. We also see a more agreeable correspondence with the logarithmic derivative curve, Figure 5, which easily displays small differences in  $vt/R$  as this index falls from  $\eta_{\text{ST}} = 0.4$ . This  $\eta_{\text{PDS}} = \frac{3}{10}$  makes  $c_{\text{PDS}} = \frac{1}{4}$ , and we then have for  $35 t_{\text{PDS}} \gtrsim t \geq t_{\text{PDS}}$  the following analytic solution:

$$R_s = R_{\text{PDS}} \left( \frac{4}{3} t_* - \frac{1}{3} \right)^{3/10}, \quad (3.32a)$$

$$v_s = v_{\text{PDS}} \left( \frac{4}{3} t_* - \frac{1}{3} \right)^{-7/10}, \quad (3.32b)$$

where the radius and velocity at the beginning of the PDS stage are

$$R_{\text{PDS}} = 14.0 \frac{E_{51}^{2/7}}{n_0^{3/7} \zeta_m^{1/7}} \text{ pc}, \quad (3.33a)$$

$$v_{\text{PDS}} = 413 n_0^{1/7} \zeta_m^{3/14} E_{51}^{1/14} \text{ km s}^{-1}. \quad (3.33b)$$

The maximum disagreement between this analytic  $R_s$  and the simulation results is  $\lesssim 2.0\%$ . Because a power law cannot duplicate the sharp drop in  $v_s$  near the shell-formation time, and also because the shock velocity from the numerical simulation occasionally fluctuates at later times, our estimate of its accuracy is less precise, but we can say that, excluding times from  $t_* = t_{\text{sf}*}$  to  $t_* \simeq 1.9 t_{\text{sf}*}$ , the offset power-law form for  $v_s$  is usually accurate to  $\lesssim 5\%$ . We also compare with the product  $R_s^2 v_s^3$ , which is proportional to the luminosity from a fully radiative shock:

$$L = \frac{1}{2} \rho_0 v_s^2 (4\pi R_s^2) v_s; \quad (3.34)$$

any small errors in  $v_s$  or  $R_s$  would lead to large errors in  $L$ . Figure 8 signifies that our offset power-law solutions will reproduce the luminosity from the shock alone to high accuracy: with the same exclusion noted above for the velocity, the product  $R_s^2 v_s^3$  is almost always within 20% of the numerical simulation. (In our next paper [Cioffi and McKee 1988] we shall reproduce the luminosity from the entire remnant at all times.) For a final comparison, we note how Chevalier (1974) found from his numerical simulation that the initial SNR energy in units of  $10^{51}$  ergs follows  $E_{51} = 5.3 \times 10^{-8} n_0^{1.12} v_{55}^{1.40} R_{s,\text{pc}}^{3.12}$ , where  $v_{55} \equiv v_s/(10^5 \text{ cm s}^{-1})$ , and  $R_{s,\text{pc}}$  is the radius in parsecs. Equation (3.27), with  $v_i$  and  $R_i$  evaluated at the beginning of the PDS stage, and with  $\eta_{\text{PDS}} = \frac{3}{10}$ , implies

$$v_* = R_*^{-7/3}. \quad (3.35)$$

Solving equations (3.34) and (3.35) for  $E_{51}$  and writing the fractions as decimals for easier comparison, we have

$$E_{51} = 6.8 \times 10^{-8} n_0^{1.16} v_{55}^{1.35} R_{s,\text{pc}}^{3.16} \zeta_m^{0.161}, \quad (3.36)$$

which is quite similar to Chevalier's numerical result.

#### IV. LATE-TIME BEHAVIOR

When radiation has removed most of the interior thermal energy, we expect the pressure-driven snowplow to evolve into

a momentum-conserving snowplow with  $R_s \propto t^{1/4}$  (Oort 1951); furthermore, at some point the SNR should merge with the ISM, losing its identity as a dynamic interstellar structure. Just as the "memory" of the pressure in the ST stage delays and modifies the PDS stage, giving an effective  $\eta$  larger than  $\frac{2}{3}$ , so too our ODE results show that the memory of the PDS pressure delays the MCS stage. Indeed, near the end of the numerical simulation ( $t \approx 35 t_{\text{PDS}}$ ), we find that  $v_s t/R_s$  still exceeds  $\frac{2}{3}$ , and the solutions of the ODE in § IIIb show that  $v_s t/R_s$  is closer to  $\frac{2}{3}$  than  $\frac{1}{4}$  even when  $t \approx 200 t_{\text{PDS}}$ . As we shall see below, the remnant usually will have merged with the ISM long before this, so that for practical purposes *the MCS stage does not occur in the ISM.*

We note two important physical limitations in applying our late-time mathematical results: hot gas must exist in the interior, supplying the driving pressure, and the ambient pressure must remain negligible. The first criterion will be satisfied if there is gas in the remnant with a cooling time  $t_{\text{cool}}$  which exceeds the age of the remnant and thermal conduction remains negligible. For a  $T^{-1/2}$  cooling law, the cooling time is (Kahn 1976; McKee 1982):

$$t_{\text{cool}} = 6.3 \times 10^{-5} \frac{s}{\zeta_m} \text{ yr}, \quad (4.1)$$

where  $x_t = 2.3$  and  $s \equiv T^{3/2}/n$ ; the entropy per unit mass is  $(k_B/\mu) \ln s$ . (Some additional cooling by dust, and, for  $T \gtrsim 10^{7.5}$  K, by bremsstrahlung radiation, reduces the actual cooling time below this value.) The advantage of this form of the cooling time is its invariance throughout the expansion experienced by the gas inside an SNR. The blast wave imparts an entropy  $s = 1.28 \times 10^{10} v_{s8}^3/n_0 \text{ K}^{3/2} \text{ cm}^3$  to the shocked gas, where  $v_{s8} \equiv v_s/(10^8 \text{ cm s}^{-1})$ . Since the shock velocity in the ejecta-dominated stage is  $v_{ej} \approx 10^{8.5-10^9} \text{ cm s}^{-1}$ , the maximum cooling time can be quite large. Thermal conduction in the interior limits  $s$  to  $1.0 \times 10^{11} E_{51}^{3/14} \eta_0^{-4/7} \phi_c^{-9/14} \text{ K}^{3/2} \text{ cm}^3$ , where  $\phi_c$  is the ratio of the actual thermal conductivity to the Spitzer (1962) value (McKee 1982). Rather than defining the onset of the MCS stage in terms of an  $\eta = \frac{1}{4}$  law, we say that it occurs at the cooling time of the hottest gas surviving in the remnant:

$$t_{\text{MCS}*} \equiv \frac{t_{\text{MCS}}}{t_{\text{PDS}}} = \min \left[ \frac{61 v_{ej,8}^3}{\zeta_m^{9/14} n_0^{3/7} E_{51}^{3/14}}, \frac{476}{(\zeta_m \phi_c)^{9/14}} \right], \quad (4.2)$$

where the initial shock velocity of the blast is  $v_{ej,8} = 10(E_{51}/M_{ej,\odot})^{1/2}$  in terms of the ejected mass  $M_{ej,\odot}$  in solar units. For  $t > t_{\text{MCS}}$  (and  $t < t_{\text{merge}}$  as discussed below), the remnant expands at the momentum given by equation (3.25):

$$R_*^4 = 4.66(t_* - t_{\text{MCS}*})(1 - 0.779 t_{\text{MCS}*}^{-0.17}) + R_{\text{MCS}*}^4 \quad (\text{MCS}), \quad (4.3)$$

where  $R_{\text{MCS}*} \equiv R_*(t_{\text{MCS}*})$  is obtained from equation (3.26).

The second criterion which the SNR must satisfy to validate our analysis of the late-time behavior is that the interior pressure must exceed the pressure of the ambient medium, or equivalently, that the blast wave velocity  $v_s$  must exceed the ambient isothermal sound speed  $C_0$  by a factor  $\beta$  of order unity. Although the dissolution of the SNR occurs over a period of time, one can choose a particular  $\beta$  to mark the beginning of the SNR's merger with the ISM. We therefore wish to write the time and radius as a function of  $\beta$ , and although less accurate at very late times than equation (3.26),

we shall find that the early death of typical SNRs permits our use of the offset power law (3.32) for  $R_s$ . (In more extreme cases one should use the analytic ODE results, equations [3.17] which can provide a more accurate but specifically numerical answer for the merge time and merge radius under particular conditions.) Noting that  $v_{\text{PDS}} \equiv v_s(t_{\text{PDS}}) = 2R_{\text{PDS}}/5t_{\text{PDS}}$ , we find

$$t_{\text{merge}*} \equiv \frac{t_{\text{merge}}}{t_{\text{PDS}}} = \frac{3}{4} \left( \frac{v_{\text{PDS}}}{\beta C_0} \right)^{10/7} = 153 \left( \frac{E_{51}^{1/14} n_0^{1/7} \zeta_m^{3/14}}{\beta C_{06}} \right)^{10/7}, \quad (4.4a)$$

and

$$R_{\text{merge}*} \equiv \frac{R_{s,\text{merge}}}{R_{\text{PDS}}} = 4.93 \left( \frac{E_{51}^{1/14} n_0^{1/7} \zeta_m^{3/14}}{\beta C_{06}} \right)^{3/7}. \quad (4.4b)$$

For  $C_{06} \equiv C_0/(10^6 \text{ cm s}^{-1}) \approx 1$  (which is characteristic of interstellar gas with  $n_0 \approx 0.1 \text{ cm}^{-3}$  and also applies to a cloudy medium with a velocity dispersion of order  $10 \text{ km s}^{-1}$ ), and for  $E_{51} = 1$ ,  $\zeta_m = 1$ , and  $\beta = 2$ , the normalized merge time is

$$t_{\text{merge}*} = 57 n_0^{10/49}. \quad (4.5)$$

Unless the ambient density is unusually large or the ejection velocity is unusually small, this time is smaller than the MCS onset time in equation (4.2). The maximum time that the SNR can evolve and remain in the PDS stage is

$$t_{\text{max}} = \min(t_{\text{MCS}}, t_{\text{merge}}). \quad (4.6)$$

For the numerical simulation in § II, we adopted an unrealistically low value for  $C_{06}$  of 0.037 in order to eliminate the effects of the ambient medium; this corresponds to  $t_{\text{merge}*} \approx 3900$ , far beyond the time at which the simulation was terminated (and large enough that our use of eq. [4.4] for  $t_{\text{merge}*}$  is quite approximate). If conduction is ignored, we have  $t_{\text{max}} = t_{\text{merge}}$  as well. At this time  $R_{\text{max}*} \approx 11$  from equation (3.26), the index  $\eta = 0.26$ , and one can see from the graph that the momentum continues to rise, although slowly. The momentum has reached  $\approx 80\%$  of the final value determined from equation (3.25):

$$(M_s \bar{v})_{\text{final}} = 4.8 \times 10^5 \frac{E_{51}^{13/14}}{\zeta_m^{3/14} n_0^{1/7}} M_\odot \text{ km s}^{-1}. \quad (4.7)$$

We also note that if the density is very low, the SNR will merge before entering the PDS stage, i.e., before cooling has become important. If we write this criterion in terms of the pressure of the ambient medium, where  $P_4 = P/(10^4 k_B \text{ K cm}^{-3})$ , then the critical (hydrogen) density is

$$n_{\text{cr}} = 0.0038 \left( \frac{P_4^{7/9} \beta^{14/9}}{E_{51}^{1/9} \zeta_m^{1/3}} \right) \text{ cm}^{-3}, \quad (4.8)$$

and the maximum radius is

$$R_{s,\text{merge}} = 151 \left( \frac{E_{51}}{P_4 \beta^2} \right)^{1/3} \text{ pc} \quad (t_{\text{merge}*} < 1), \quad (4.9)$$

independent of the density (Cioffi 1985).

## V. CONCLUSIONS

We can treat the evolution of a supernova remnant in a simple analytic manner because the complications revealed by

the details of our hydrodynamical simulation do not greatly affect the global propagation of the blast wave, although they may affect its appearance. For example, weak shocks left over from the reverse shock scatter repeatedly off the ejecta and scramble the thermal structure so much that the Sedov-Taylor similarity solution never obtains. We also observe that the formation of the dense shell is a complex hydrodynamical event which perhaps cannot be properly modeled in a one-dimensional calculation.

Thus, with particular attention to the dynamics of the SNR during shell formation, we have introduced an improved offset power-law analytic solution, equation (3.32), for the pressure-driven expansion of a supernova remnant into a homogeneous, uniform medium. This solution matches our hydrodynamical simulation, showing a smoothly varying logarithmic derivative after the end of the Sedov-Taylor stage and giving the radius to within a few percent for  $35 t_{\text{PDS}} \gtrsim t > t_{\text{PDS}}$ . We use an effective power-law exponent in the PDS stage of 0.30 rather than  $\frac{2}{3}$ .

We have developed a simple pair of ordinary differential equations (3.17) which describes the evolution of a blast wave with radiative losses. With a suitable approximation for the interior pressure, we numerically integrated these equations and duplicated the kinematical behavior seen in our hydrodynamical simulation. Further approximations enabled us to obtain an analytic solution to these equations, equation (3.26),

which matches the numerical solution to very late times. The late-time solution is particularly useful for determining the evolution of remnants in moderately dense media. These solutions describe the PDS stage of SNR evolution, which ends either when the internal driving pressure vanishes due to radiative cooling or when the remnant merges with the ambient ISM. In the first case, the remnant would enter the momentum-conserving snowplow stage with  $R_s \propto t^{1/4}$ . We have found that SNRs generally merge with the ISM before they can enter this stage, however. In a subsequent paper, we give the details of our cooling calculations and provide an analytic calculation of the luminosity from all stages, which again agrees well with hydrodynamical simulations.

We thank Don Cox for comments which substantially improved the paper. This work has been supported through NSF grants AST 83-14684 and AST 86-15177. All computations, other than the hydrodynamical simulation itself, were carried out on a Tandy 2000 HD generously awarded by the Tandy Corporation. D. F. C. thanks Dr. Cheng Ho for much assistance, and Dr. Rosemary Wyse for many helpful discussions. E. B. thanks the Miller Institute for Basic Research in Science at U. C. Berkeley for their support during part of this project.

## REFERENCES

- Bertschinger, E. 1986, *Ap. J.*, **304**, 154.  
 Chevalier, R. A. 1974, *Ap. J.*, **188**, 501.  
 Cioffi, D. F. 1985, Ph.D. thesis, University of Colorado.  
 Cioffi, D. F., and McKee, C. F. 1988, in preparation.  
 Collela, P., and Woodward, P. R. 1984, *J. Comput. Phys.*, **54**, 174.  
 Cox, D. P. 1972, *Ap. J.*, **178**, 159.  
 ———. 1986, *Ap. J.*, **304**, 771.  
 Cox, D. P., and Anderson, P. R. 1982, *Ap. J.*, **253**, 268.  
 Cox, D. P., and Edgar, R. J. 1983, *Ap. J.*, **265**, 443.  
 Dwek, E. 1981, *Ap. J.*, **247**, 614.  
 Falle, S. A. E. G. 1981, *M.N.R.A.S.*, **195**, 1011.  
 Gaffet, B. 1978, *Ap. J.*, **225**, 442.  
 ———. 1983, *Ap. J.*, **273**, 267.  
 Graham, J. R., Evans, A., Albinson, J. S., Bode, M. F., and Meikle, W. P. S. 1987, *Ap. J.*, **319**, 126.  
 Gull, S. F. 1973, *M.N.R.A.S.*, **161**, 47.  
 Ikeuchi, S., and Spitzer, L. 1984, *Ap. J.*, **283**, 825.  
 Innes, D. E., Giddings, J. R., and Falle, S. A. E. G. 1987, *M.N.R.A.S.*, **226**, 67.  
 Kahn, F. D. 1976, *Astr. Ap.*, **145**, 50.  
 Landau, L. D., and Lifshitz, E. M. 1959, *Fluid Mechanics* (Oxford: Pergamon).  
 Lapidus, A. 1967, *J. Comput. Phys.*, **2**, 154.  
 Mansfield, V. N., and Salpeter, E. E. 1974, *Ap. J.*, **190**, 305.  
 McKee, C. F. 1974, *Ap. J.*, **188**, 335.  
 McKee, C. F. 1982, in *Supernovae: A Survey of Current Research*, ed. M. Rees and R. Stoneham (Dordrecht: Reidel), p. 433.  
 McKee, C. F., and Ostriker, J. P. 1977, *Ap. J.*, **218**, 148.  
 Oort, J. H. 1951, in *Problems of Cosmical Aerodynamics* (Dayton, Ohio: Central Air Document Office), p. 118.  
 Ostriker, J. P., and McKee, C. F. 1988, *Rev. Mod. Phys.*, **60**, 1.  
 Ostriker, J. P., and Silk, J. 1973, *Ap. J. (Letters)*, **184**, L71.  
 Raymond, J. C., Cox, D. P., and Smith, B. W. 1976, *Ap. J.*, **204**, 290.  
 Richtmeyer, R. D., and Morton, K. W. 1967, *Difference Methods for Initial-Value Problems* (New York: Wiley-Interscience).  
 Sedov, L. I. 1959, *Similarity and Dimensional Methods in Mechanics* (New York: Academic).  
 Shull, J. M. 1980, *Ap. J.*, **237**, 769.  
 Sod, G. A. 1978, *J. Comput. Phys.*, **27**, 1.  
 Solinger, A., Rappaport, S., and Buff, J. 1975, *Ap. J.*, **201**, 381.  
 Spitzer, L. 1978, *Physical Processes in the Interstellar Medium* (New York: Wiley-Interscience).  
 ———. 1982, *Ap. J.*, **262**, 315.  
 Straka, W. C. 1974, *Ap. J.*, **190**, 59.  
 Taylor, G. I. 1950, *Proc. Roy. Soc. London A*, **201**, 159.  
 Wheeler, J. C., Mazurek, T. J., and Sivaramakrishnan, A. 1980, *Ap. J.*, **237**, 781.  
 Woltjer, L. 1972, *Ann. Rev. Astr. Ap.*, **10**, 129.

EDMUND BERTSCHINGER: Department of Physics, MIT, Room 6-207, Cambridge, MA 02139

DENIS F. CIOFFI: NASA/Goddard Space Flight Center, Laboratory for High Energy Astrophysics, Code 665, Greenbelt, MD 20771

CHRISTOPHER F. MCKEE: Physics Department, University of California, Berkeley, CA 94720.